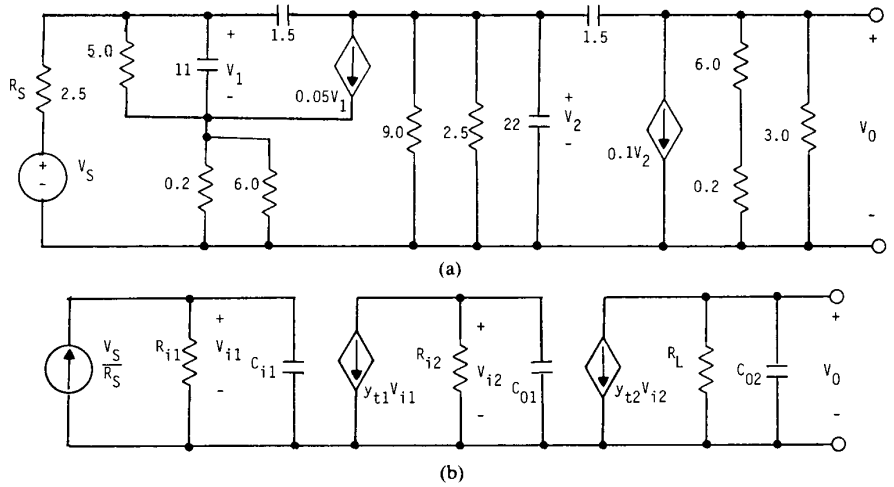

Fig. 4. (a) The equivalent circuit of an amplifier shown in [3, fig. 13.9(b), p. 598]. (b) Its unilateral model. All resistances in kiloohms and capacitances in picofarads.

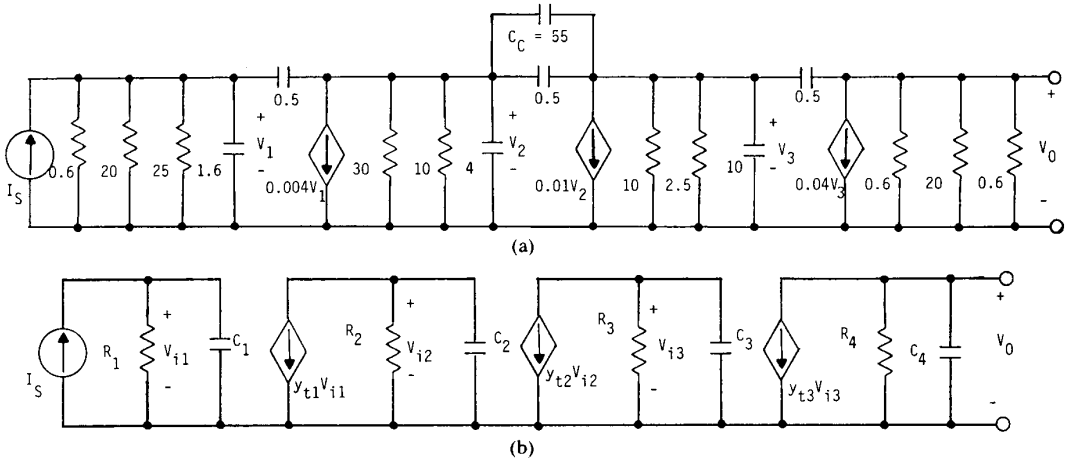

Fig. 5. (a) The equivalent circuit of an amplifier shown in [3, fig. 13.17, p. 593]. (b) Its unilateral model. All resistances are in kiloohms and capacitances in picofarads.

critical frequencies of the circuits. This point is clearly illustrated by both examples taken from [3]. Because of the good accuracy of the methods presented in this paper, we can use this method in various applications of amplifier circuits, such as determining the bandwidth, stability, stability margins and closed-loop poles, etc.

Acknowledgment

The author wishes to thank Dr. P. K. Rajan and some unknown reviewers for their constructive comments and suggestions to improve the quality of this paper.

References

[1] Adel S. Sedra and Kenneth C. Smith, *Microelectronic Circuits*. New York: Holt, Rinehart and Winston, 1987 (second edition).
[2] M. S. Ghausi, *Electronic Devices and Circuits*, New York: Holt, Rinehart and Winston, 1985.
[3] Jacob Millman and Arvin Grabel, *Microelectronics*. New York: McGraw Hill, 1987 (second edition).
[4] B. L. Cochrun and A. Grabel, "A method for the determination of the transfer function of electronic circuits," *IEEE Trans. Circuits Syst.*, vol. CT-20, Jan. 1973.
[5] A. M. Davis and E. A. Moustakas, "Analysis of active *RC* networks by decomposition," *IEEE Trans. Circuits Syst.*, vol. CAS-27, pp. 417–419, May 1980.
[6] Douglas N. Green, "An improved Miller Effect Model for high frequency behavior," *IEEE Trans. Education*, vol. E-28, pp. 125–130, Aug. 1985.

Multidimensional Projection Windows

WEN-CHUNG STEWART WU, KWAN F. CHEUNG, AND ROBERT J. MARKS, II

***Abstract*—A one-dimensional window is chosen from the large catalog of those available primarily due to its leakage-resolution tradeoff (LRT). Is it possible to generalize a 1-D window to higher dimensions such that the**

Manuscript received June 6, 1987; revised February 18, 1988. This paper was recommended by Associate Editor D. M. Goodman.

The authors are with Interactive Systems Design Laboratory, University of Washington at Seattle, Seattle, WA 98195.

IEEE Log Number 8822405.

window's 1-D properties are homogeneously preserved? If we require that the window be continuous and bounded the answer is usually no. Bounded (projection window) generalizations do exist for the Parzen and Tukey–Hanning windows. The resulting windows, however, are very close to that window obtained by simply rotating the 1-D window into two dimensions.

Introduction

When choosing from the large catalog of standard 1-D windows [1]–[2], one is largely motivated by the window's leakage-resolution tradeoff (LRT). Is it possible to generalize these windows to two and higher dimensions such that the 1-D window properties are preserved in each 1-D slice? If we require these multidimensional windows to be bounded and continuous, the answer is usually negative. In the two cases considered in this correspondence where bounded 2-D generalizations do exist, the resulting windows are close to those obtained by the rotation generalization of 1-D windows [3].

A short review of the outer product and rotation of 1-D window generalization methods is given in the next section. In both cases, the LRT is altered in the transformation. In order to homogeneously maintain the 1-D window properties, the higher dimension window must be chosen so that its projection onto one dimension results in the 1-D window. Unfortunately, this requires unbounded generalizations in many cases of interest. The Parzen and Tukey–Hanning windows are exceptions. For the discrete case, bounded projection windows can be formed such that desired LRT is preserved inhomogeneously at a number of angular orientations.

Preliminaries

There are an wealth of 1-D windows with various LRT's. A 1-D window, $w_1(t)$ has finite extent:

$$w_1(t) = w_1(t)\,\Pi(t/2\tau)$$

(where $\Pi(t) = 1$ for $|t| \leqslant 1/2$ and is zero elsewhere), is normalized with

$$w_1(0) = 1$$

and is an even function, i.e.,

$$w_1(t) = w_1(-t).$$

The spectrum of a window is defined by

$$W_2(\omega) = \int_{-\infty}^{\infty} w_1(t) \exp(-j\omega t)\, dt.$$

The area of a window is

$$A = \int_{-\infty}^{\infty} w_1(t)\, dt = W_1(0).$$

The magnitude of a typical window spectrum is shown in Fig. 1. For good resolution, the main lobe width, Δ, should be small, and for minimal spectral leakage, the normalized side lobe magnitude, δ, should also be small. Invariably, however, decreasing one of these parameters increases the other.

A 2-D window $w_2(t_1, t_2)$, with spectrum

$$W_2(\omega_1, \omega_2) = \int_{-\infty}^{\infty}\int_{-\infty}^{\infty} w_2(t_1, t_2) \exp[-j(\omega_1 t_1 + \omega_2 t_2)]\, dt_1\, dt_2$$

is commonly generated from a 1-D counterpart by either the outer product or window rotation techniques [3]. The outer product window is

$$w_2^{op}(t_1, t_2) = w_1(t_1)\, w_1(t_2)$$

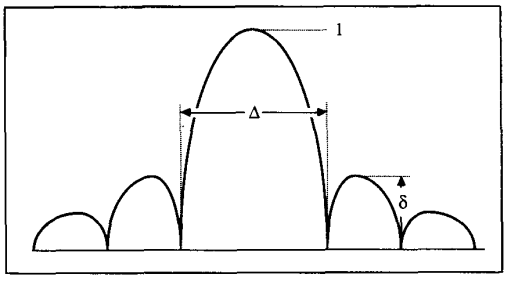

Fig. 1. The normalized spectrum of a typical 1-D window, $|W_1(\omega)|/A$. The values of Δ and δ parameterize the window's resolution and leakage, respectively.

and the rotated window, initially suggested by Huang [4], is

$$w_2^{rw}(t_1, t_2) = w_1\left(\sqrt{t_1^2 + t_2^2}\right).$$

In either case, if w_1 is a "good" window, then so is w_2. For certain applications, (e.g., "good" filter design) such dimensional generalizations are acceptable. In other cases, such as spectral estimation, a small perturbation in window shape can significantly alter results [5]. Both the outer product and the rotated window significantly alter the LRT of the corresponding 1-D window.

To illustrate the effects of outer product and rotational dimensional generalization, we choose a boxcar window

$$w_1(t) = \Pi(t/2\tau).$$

It follows that

$$W_1(\omega) = 2\sin(\tau\omega)/\omega$$

for which

$$\Delta = 6.3/\tau; \quad \delta = 0.22. \tag{1}$$

For the outer product window, in general,

$$W_2^{op}(\omega_1, \omega_2) = W_1(\omega_1)\, W_2(\omega_2).$$

The result is a window with an identical LRT as the 1-D window in the t_1 and t_2 directions. Indeed

$$W_2(\omega_1, 0) = A\, W_1(\omega_1).$$

However, in other directions, the LRT can be significantly altered. For example, in the (t_1, t_2) plane, the Δ parameter for the window resolution in the $\pm 45°$ directions in $\sqrt{2}$ times that of the $0°$ and $90°$ directions. Consider, specially, the boxcar window, for which

$$W_2(\omega_1, \omega_2) = 4\sin(\tau\omega_1)\sin(\tau\omega_2)/(\omega_1\omega_2).$$

The 1-D slice of this window along the $45°$ diagonal is

$$W_2^{op}\left(\omega_1/\sqrt{2}, \omega_2/\sqrt{2}\right) = 4\sin^2\left(\omega/\sqrt{2}\right)/\omega^2$$

which is the spectrum of a Bartlett (triangular) window. The parameters of this window with respect to those in (1) are

$$\Delta_{45°} = \sqrt{2}\,\Delta \cong 8.9/\tau$$

and

$$\delta_{45°} = 0.047 \cong (0.22)^2 = \delta^2.$$

Clearly, the LRT is significantly altered.

For the rotated window, the window spectrum can be written as

$$W_2^{rw}(\omega_1, \omega_2) = W_2(\rho) = 2\pi\int_0^{\infty} r W_1(r) J_0(r\rho)\, dr \tag{2}$$

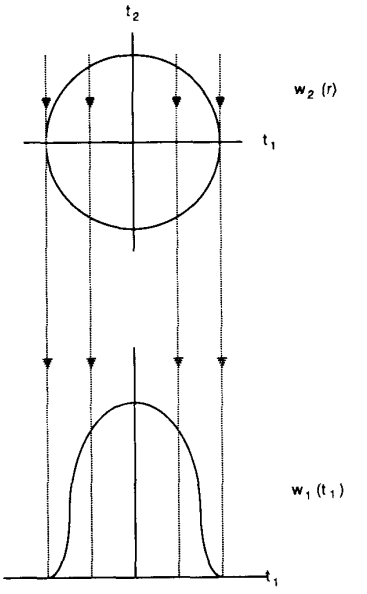

Fig. 2. Illustration of the mechanics of forming a 1-D projection, $w_1(t_1)$, from a 2-D circularly symmetric function $\hat{w}_2(r)$, $(r^2 = t_1^2 + t_2^2)$. If $w_1(t_1)$ is the projection of $w_2(r)$, then $w_2(r)$ homogeneously preserves the LRT of its 1-D counterpart.

where

$$\rho = \sqrt{\omega_1^2 + \omega_2^2}$$

and

$$r = \sqrt{t_1^2 + t_2^2}.$$

Equation (2) is the familiar Hankel transform [6] which results from Fourier transforming a circularly symmetric 2-D function. Although the rotation window does not have the directional inhomogeneity of the outer product window, the LRT of the original window is also significantly altered. Consider the rotated boxcar window with spectrum

$$W_2^{rw}(\rho) = 2\pi\tau J_1(\tau\rho)/\rho.$$

Here

$$\Delta_{rw} \cong 7.7/\tau = 1.2\,\Delta$$

and

$$\delta_{rw} = 0.13 \cong 0.59\,\delta.$$

The Projection or Rotated Spectrum Window

The 2-D window, $w_2^p(r)$, that preserves the LRT of its corresponding 1-D window in all directions will be referred to as the projection or rotated spectrum window. The window can be thought of in one of two equivalent ways:

1) Projection

With reference to Fig. 2, $w_2^p(r)$ is the window whose projection is the 1-D design window,

$$w_1(t_1) = \int_{-\infty}^{\infty} w_2^p(r)\, dt_2. \tag{3}$$

By straightforward manipulation, w_1 is recognized as the Abel transform of w_2^p:

$$w_1(t_1) = 2\int_{t_1}^{\infty} r w_2^p(r)/\sqrt{r^2 - t_1^2}\, dr.$$

Thus the 2-D window can be obtained from an inverse Abel transform [6]:

$$w_2(r) = \frac{1}{\pi}\int_r^{\infty} \sqrt{t_1^2 - r^2}\, \frac{d}{dt_1}\left(\frac{w_1'(t_1)}{t_1}\right) dt_1$$

where the prime denotes differentiation. Since $w_1(t_1)$ is zero for $|t_1| > \tau$, an equivalent expression is [6]:

$$w_2(r) = \frac{1}{\pi}\int_r^{\infty} \sqrt{t_1^2 - r^2}\, \frac{d}{dt_1}\left(\frac{w_1'(t_1)}{t_1}\right) dt_1 - \frac{w_1'(\tau)}{\pi\tau}\sqrt{\tau^2 - r^2}, \quad \text{for } |r| \leqslant \tau. \tag{4}$$

2) Rotated Spectrum

The spectrum of the projection window is the rotation of the spectrum of the 1-D window. That is,

$$W_2^p(\rho) = W_1(\rho).$$

The window can thus be obtained by an inverse Hankel transform:

$$w_2^p(r) = \int_0^{\infty} \rho W_1(\rho) J_0(r\rho)\, d\rho/2\pi.$$

Through this definition of projection window, one can clearly see that the LRT of the original window is preserved in the 2-D generalization in all directions.

The equivalence of this and the projection window follows immediately from the continuous version of the projection-slice theorem [3] or, for even functions, from the equality of an Abel transform to Fourier Transform followed by an inverse Hankel transform [6].

Examples

1) The *Parzen Window* is obtained by convolving two identical (Bartlett type) triangular windows and normalizing. The result is [7]

$$w_1(t_1) = \begin{cases} 1 - 6\left(\dfrac{t_1}{\tau}\right)^2 + 6\left|\dfrac{t_1}{\tau}\right|^3, & |t_1| \leqslant \tau/2 \\ 2\left(1 - \left|\dfrac{t_1}{\tau}\right|\right)^3, & \tau/2 \leqslant |t_1| \leqslant \tau \\ 0, & |t_1| \geqslant \tau. \end{cases}$$

Recognizing that $w_1'(\tau) = 0$, we obtain from (4) after some variable substitution:

$$\hat{w}_2(r) = w_2^p(r\tau) = \begin{cases} \dfrac{9}{\pi}\left(\dfrac{b}{2} - r^2 \ln\left(\dfrac{\frac{1}{2} - b}{r}\right)\right) + \dfrac{6}{\pi}\left(\dfrac{9b}{4} - \dfrac{3a}{2} + c\ln\left(\dfrac{1+a}{\frac{1}{2}+b}\right)\right), & 0 \leqslant r \leqslant \dfrac{1}{2} \\ \dfrac{6}{\pi}\left(\dfrac{-3a}{2} + c\ln\left(\dfrac{1+a}{r}\right)\right), & \dfrac{1}{2} \leqslant r \leqslant 1 \end{cases}$$

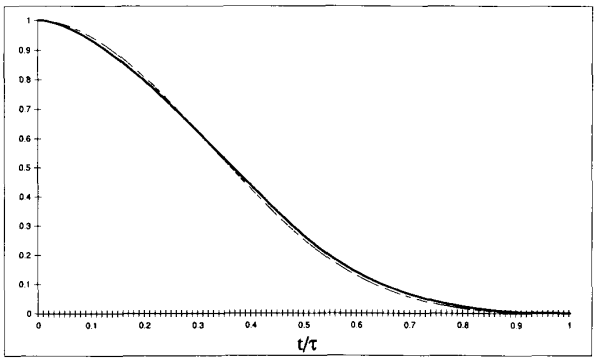

Fig. 3. Plots of the Parzen window (dashed line), and its corresponding projection window (solid line).

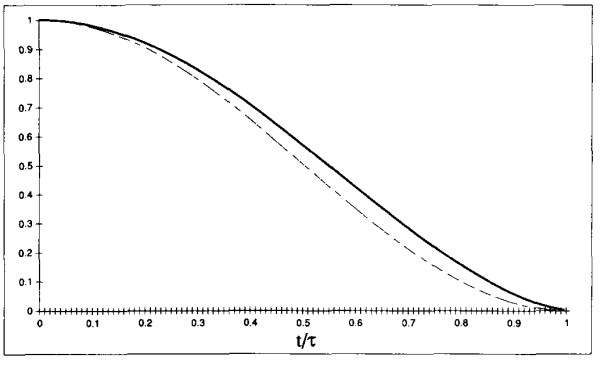

Fig. 4. Plots of the Tukey–Hanning window (dashed line), and its corresponding projection window (solid line).

where

$$a = (1 - r^2)^{1/2}$$

$$b = \left(\frac{1}{4} - r^2\right)^{1/2}$$

$$c = 1 + \frac{r^2}{2}.$$

Plots of $\hat{w}_2(r)/w_2(0)$ and $w_1(t_1)$ (for $\tau = 1$) are shown in Fig. 3 using dashed and solid lines, respectively. The difference between the two plots is nearly indistinguishable. Thus the projection and rotation windows for the Parzen window are nearly identical.

2) The *Tukey–Hanning Window* is defined as

$$w_1(t) = \frac{1}{2}\left(1 + \cos\left(\frac{\pi t}{\tau}\right)\right)\Pi(t/2\tau).$$

Recognizing that $w_1'(\tau) = 0$, we can evaluate the resulting integral in (4) to obtain $w_2^p(r)$. Normalizing gives

$$\hat{w}_2(r) = w_2^p(r\tau)/\tau$$

$$= \frac{1}{2}\int_r^1 (\xi^2 - r^2)^{1/2} \frac{\pi\xi\cos(\pi\xi) - \sin(\pi\xi)}{\xi^2}\, d\xi.$$

The integral can be easily evaluated numerically. Plots of $\hat{w}_2(r)/w_2(0)$ and $w_1(t_1)$ are shown in Fig. 4. The projection and rotation windows are again very similar.

Boundedness of the Projection Window

A problem with certain continuous projection windows is their unboundedness. For example, the projection window corresponding to the boxcar window is

$$w_2(r) = \frac{1}{\pi(\tau^2 - r^2)^{1/2}}\Pi(r/2\tau).$$

This result is unbounded around the ring $r = \tau$. Similarly, for the Bartlett (triangular) window, we obtain

$$w_2(r) = \frac{1}{\pi\tau}\cosh^{-1}(\tau/r)\,\Pi(r/2\tau).$$

This result is unbounded at the origin. Sufficient conditions for $w_2^p(r)$ to be bounded are

$$\frac{d}{dt}\left(\frac{w_1'(t)}{t}\right) < \infty \tag{5}$$

and

$$\left.\frac{dw_1(t)}{dt}\right|_{t=\tau} < \infty \tag{6}$$

These conditions follow immediately upon inspection of (4). Equation (5), for example, is violated by the Bartlett window. Equation (6) excludes all 1-D windows that are discontinuous at $t = \tau$ (e.g., Hamming and Kaiser). The necessity of this can be seen in Fig. 2. As in the vertical slice of $w_2^p(r)$ approaches $t = \tau$ from the left, the circular support requires diminishingly smaller intervals of integration. The value of $w_1(\tau^-)$ is determined by integration over an epsilon interval. Thus, in order for $w_1(\tau^-)$ to be nonzero, $w_2^p(\tau^-)$ must be infinite.

For digital signal processing, the boundedness of the projection window need not be a problem. Here, the 2-D window is set up in some given periodic grid (e.g., rectangular or hexagonal). The values in the window are chosen such that their projections [3] are the desired 1-D windows. A number of projection directions can be used. The result is a set of algebraic equations that can be solved to determine the values of the 2-D window. A second technique is to form a 2-D inverse FFT on the sampled window's rotated spectrum. Some preliminary work in such digital extensions has been done by Wu [8].

Extension to Higher Dimensions

For an N-D projection window, we wish to find $w_N(r_N)$ such that

$$w_1(r_1) = \int_{t_2}\int_{t_3}\cdots\int_{t_N} w_N(r_N)\, dt_N \cdots dt_3\, dt_2 \tag{7}$$

where $w_1(r_1)$ is a specified 1-D window and

$$r_N^2 = \sum_{k=1}^{N} t_k^2.$$

The integration in equation (7) can be done in stages, the N-th of which is

$$w_{N-1}(r_{N-1}) = \int_{t_N} w_N(r_N)\, dt$$

$$= \int_{t_N} w_N\left(\sqrt{r_{N-1}^2 + t_N^2}\right) dt_N.$$

Comparing with (3), we conclude that $w_{N-1}(r_{N-1})$ is the Abel transform of $w_N(r_N)$. Thus to generate $w_N(r_N)$, we simply need to perform $N-1$ inverse Abel transforms on $w_1(t_1)$.

A pedagogical $N=5$ closed-form example, taken directly from an Abel transform table [6], is

$$w_1(r_1)=\left[1-\left(\frac{r_1}{\tau}\right)^2\right]\Pi(r_1/2\tau)$$

$$w_2(r_2)=\frac{2}{\pi\tau^2}\left(\tau^2-r_2^2\right)^{1/2}\Pi(r_2/2\tau)$$

$$w_3(r_3)=\frac{1}{\pi\tau}\Pi(r_3/2\tau)$$

$$w_4(r_4)=\frac{1}{(\pi\tau)^2\left(\tau^2-r_4^2\right)^{1/2}}\Pi(r_4/2\tau)$$

$$w_5(r_5)=\frac{2}{\pi^2\tau}\delta(r_5-\tau)$$

where δ is the unit impulse function.

An alternate approach to multidimensional projection windows follows from the property that the inverse Hankel transform of a Fourier transform is equivalent to an Abel transform. Thus, the $(N-1)$ inverse Abel transform can be performed in the Fourier domain. Bracewell [6] has shown that these operations can be condensed into the single transform:

$$w_N(r_N)=\frac{N}{(2\pi r_N)^{N/2}}\int_0^\infty W_1(\omega)J_{N/2-1}(\omega r_N)\omega^{N/2}\,d\omega$$

where $J_{(N/2)-1}$ is the Bessel function of order $(N/2)-1$.

Conclusions

The projection window preserves the LRT of the 1-D window from which it is designed. This is not in general true for the outer product and rotation window generalizations. The Parzen and Tukey–Hanning windows were shown to have straightforward 2-D projectional window equivalents. Many other commonly used windows, however, were shown to have unbounded projection. Further work in the digital equivalent of the dimensional generalization is in order. Here, boundedness need not be an issue.

References

[1] A. V. Oppenheim and R. W. Schafer, *Digital Signal Processing*. Englewood Cliffs, NJ: Prentice-Hall, 1975.

[2] A. Papoulis, *Signal Analysis*. New York: McGraw-Hill, 1977.

[3] D. E. Dudgeon and R. M. Mersereau, *Multidimensional Digital Signal Processing*. Englewood Cliffs, Prentice-Hall, 1984.

[4] T. S. Huang, "Two dimensional windows," *IEEE Trans. Audio Electroacoust.*, vol. AU-20, pp. 88–89, 1972.

[5] F. J. Harries, "On the use of windows for harmonic analysis with the discrete fourier transform," *Proc. IEEE*, vol. 66, pp. 26–50, 1978.

[6] R. N. Bracewell, *The Fourier Transform and its Applications*. 2nd edition, (revised) New York: McGraw-Hill, 1986.

[7] M. B. Priestley, *Spectral Analysis and Time Series*. New York: Academic, 1981.

[8] W.-C. S. Wu, "Multidimensional Windows Design Using Abel Projection," Master thesis, Univ. Washington, Seattle, 1985.

Design of a Fast Variable-Frequency Josephson Shift Register

V. NANDAKUMAR AND T. VAN DUZER

Abstract—**The design of a very high speed Josephson junction shift register is presented. Computer simulations show that the circuit can be operated with a two-phase sinusoidal clock at frequencies over 60 GHz.**

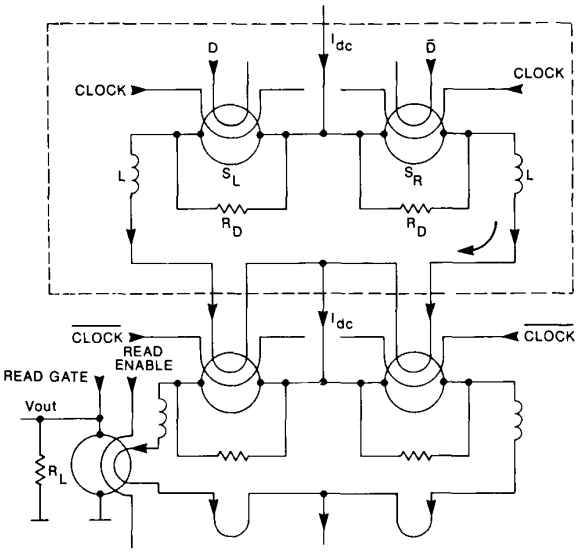

Fig. 1. One bit of the shift register comprises four writing SQUID's and one Read SQUID. The dashed box encloses a cell using one clock phase. $R_D=12\ \Omega$, $L=7.15$ pH, $R_L=12\ \Omega$, $I_{dc}=145\ \mu$A. For signal values, see Fig. 3.

The shift register is based on using nonlatching superconducting interferometric switches to shift a bias current between arms of superconducting loops. The operating margins of the circuit are discussed.

I. Introduction

Various shift registers using Josephson junctions have been proposed [1]–[3]. Some of them, although fast, employ complicated clocking schemes—they require clock waveforms that have very fast rise times, necessitating regulator junctions in-chip, and/or they need three-phase clocks, which, if generated by on-chip delay lines, fix the operating frequency. The present design allows the use of a two-phase sinusoidal clock, which is easily generated at room temperature or on-chip using a transformer. A similar idea was proposed by Matisoo and Yao [4]. Their design differs from ours in using single junctions as switching devices and with a different clocking scheme. A shift register such as the one discussed here can be used as a serial memory in a signal processing system, employing subsystems such as the 20-GHz clock rate analog-to-digital converter whose design is described in [5]. An important requirement for a fast serial memory, fulfilled by the present design, is the capability of reading the data without interrupting the clock.

II. Circuit Description

Fig. 1 shows the schematic of one bit of the shift register. Each bit consists of two identical cells; the first cell is shown enclosed by broken lines. A superconducting line carrying a dc current I_{dc}, which splits into two identical branches, feeds all cells in series. Each branch has in it a superconducting quantum interference

Manuscript received August 25, 1987; revised January 4, 1988. This work was supported by the Office of Naval Research under Contract N00014-77-C-0419. This paper was recommended by Associate Editor C. A. T. Salama.

The authors are with the Department of Electrical Engineering and Computer Science, Electronics Research Laboratory, University of California, Berkeley, CA 94720.

IEEE Log Number 8822406.